RSC Advances

Volume 1 | Number 1 | Jan 2013 | Pages 1–100

RSC Advances

www.rsc.org/advances

ROYAL SOCIETY OF CHEMISTRY

ROYAL SOCIETY OF CHEMISTRY

www.rsc.org/advances

Cite this: DOI: 10.1039/c0xx00000x

www.rsc.org/xxxxxx

ARTICLE TYPE

From solid carbon sources to carbon nanotubes: a general water-assisted approach

Su Zhang[1], Lei Qin[1], Huaihe Song*, Xiaohong Chen, Jisheng Zhou, Zhaokun Ma

Received (in XXX, XXX) Xth XXXXXXXXX 20XX, Accepted Xth XXXXXXXXX 20XX
DOI: 10.1039/b000000x

We reported a universal approach to prepare carbon nanotubes from solid-state carbons. Under the assistance of trace amount of water vapor, efficient growth of kinds of carbon nanotubes were achieved from commercially available artificial graphite powder, carbon black and amorphous carbon powder under a relative low temperature of 850 ˚C. This present method provided a new horizon for effective utilization of low value added carbon resources to fabricate advanced carbon materials and could help to deeply understand the structure transformation of solid carbon materials.

1. Introduction

Due to the unique one-dimensional structure and excellent physicochemical properties, carbon nanotube (CNT) occupied very important position in advanced technical applications such as energy storage, machinery, composites and chemical engineering[1-5]. Preparation of CNT is not a new topic so far since kinds of routes were extensively investigated in the previous works, such as arc-discharge evaporation, laser-vaporization, chemical vapor deposition (CVD), and catalytic thermal decomposition.[2, 6-9] Among them, the earlier invented arc-discharge evaporation and laser vaporization methods can successfully transform solid state carbon precursors to high crystal CNTs, but severe synthesis conditions such as ultrahigh reaction temperature, high vacuum and voltage are required during these procedures[7, 8]. In contrast, CVD method nowadays are considered as the most convenient and efficient route for large-scale and controllable fabrication of CNTs because under the assistance of catalytic transition metal nanoparticles, growth of CNTs can be easily achieved using carbon enriched gases as the precursors[2, 7, 8]. However, along with the increasingly serious resource, environmental and energy problems worldwidely, to satisfy the efficient utilization of chemical resources, simple approaches for large-scale preparation of various CNTs from low value-added carbon precursors are still urgently demanded. Previously, our group proposed that carbon nanofibers can be prepared from solid state carbons under the treated temperature of 1500 ˚C[10]. Biris et. al. reported that graphene could be converted into CNT via gold nanoparticles under relative low temperatures [11]. But as far as we know, preparation of CNTs from solid carbon sources is still a great challenge till now.

Herein, we put forward that under the assistance of trace amount of water, herringbone and cylinder like CNTs can be obtained from various solid phase carbon sources at a relative low temperature of 850 ˚C using NiO-MgO as the catalyst. Water can maintain the activity of the catalysts in CVD method by suppressing the Ostwald ripening between transition metal nanoparticles and preventing the deposition of amorphous carbons[8, 12-18]. In our approach, water can also promote the growth process by maintaining the catalytic activity of Ni nanoparticles and activating the solid carbon simultaneously, thus ensured the efficient transformation of solid carbon resources to CNTs. Our work provides a promising way to fabricate advanced carbon materials using low value-added carbon raw materials and it could further contribute to build up novel perspectives on the relationships and correlated structural transformation mechanisms between different solid state carbons.

2. Experimental Section:

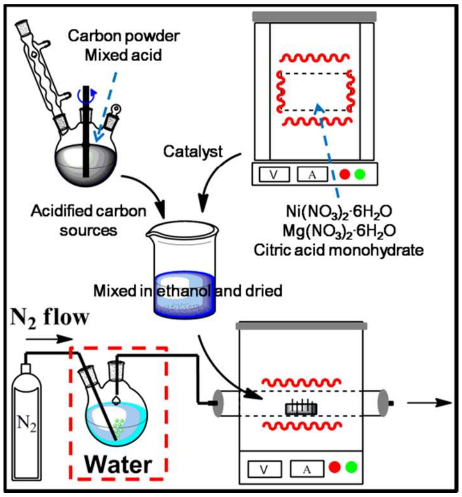

Figure 1 sketch for the water-assisted growth of CNTs using various solid-state carbon sources.

State Key Laboratory of Chemical Resource Engineering, Beijing Key Laboratory of Electrochemical Process and Technology for Materials, Beijing University of Chemical Technology, Beijing, 100029, P. R. China. Fax: +86- 10- 6443-4916; Tel: +86- 10- 6443-4916;
E-mail: songhh@mail.buct.edu.cn

2.1 Materials and Chemical Agents:

The commercial available amorphous carbon powder (Qingdao Auke graphite Co., Ltd., Qingdao, China), carbon black (Mitsubishi Chemical Corporation, 24 nm), and artificial graphite (Qingdao Auke graphite Co., Ltd., Qingdao, China) were carried out as the solid carbon precursors in this work. All the chemical agents we utilized are analytical pure without further purification. The electric resistance of the deionized water is 18.2 MΩ.

2.2 Acidification of carbon sources:

The sketch for the preparation route was given in Figure 1. For the acidification of the solid carbon precursors, 5 g of the solid carbon were separated into the mixed acid composed of 90 ml of H_2SO_4 (98 wt %) and 30 ml of HNO_3 (70 wt %) and then refluxed at 80 ˚C for 70 h. The product were washed to neutral by deionized water and dried at 80 ˚C in a vacuum oven.

2.3 Preparation of NiO-MgO catalyst:

For the synthesis of NiO-MgO catalyst, 4 g of the $Ni(NO_3)_2·6H_2O$, 1.76 g of the $Mg(NO_3)_2·6H_2O$, and 4.33 g of the citric acid ($C_6H_8O_7·H_2O$) were dissolved in 100 ml of ethanol with stirring for 6 h. The mixture was dried at 80 ˚C with stirring till green syrup was obtained. The black catalyst powder was further prepared by annealing the green syrup (kept in a 100 ml corundum crucible) in a muffle oven at 400 ˚C for 3 h under air atmosphere.

2.4 Preparation of CNTs:

The as-prepared catalyst (0.100 g) and acidified carbon source (0.030 g) was firstly mixed in 50 ml of ethanol with strong stirring for 3 h and then dried at 80 ˚C in a vacuum oven. Subsequently, the solid mixture was put into a tube furnace and under the protection of N_2 atmosphere (0.2 L min^{-1}, 25 ˚C), the annealed temperature was raised to 500 ˚C by 2 ˚C min^{-1}. At this point, trace amount of water vapor was introduced into the furnace by N_2 gas flow (0.2 L min^{-1}, 25 ˚C) and the temperature was raised to 850 ˚C by 5 ˚C min^{-1}. Then, the furnace was allowed to cool down to room temperature with the rate of 5 ˚C min^{-1}. For comparison, the growth process was taken using the same ratio of acidified artificial graphite and catalyst mixture under the same experimental condition without the introduction of water vapor.

To remove the catalyst particles from the obtained products, 0.1 g of the products, 50 ml of HCl (38 wt %), and 10 ml of the H_2O_2 (30 wt %) was mixed and stirred at room temperature for 4 h. The CNTs were washed to neutral by deionized water and dried at 80 ˚C.

2.5 Characterization:

The morphologies of the obtained samples were carried out by scanning electron microscopy (SEM, FE-JSM-6701F) and high resolution transmission electron microscopy (HRTEM, JEOL-2100F). The crystal structures of the samples were measured by X-ray diffraction (XRD) recorded on a Rigaku D/max-2500B2+/PCX system operating at 40 kV and 20 mA using Cu Kα radiation. Raman spectroscopy was carried out using a 532 nm laser (Aramis, Jobin Yvon). The samples were prepared by dispersing in ethanol with soft sonication and dropped the dispersion on SiO_2/Si substrate, then dried it at room temperature. For each sample we measured at least 3 different points.

3. Results and Discussion:

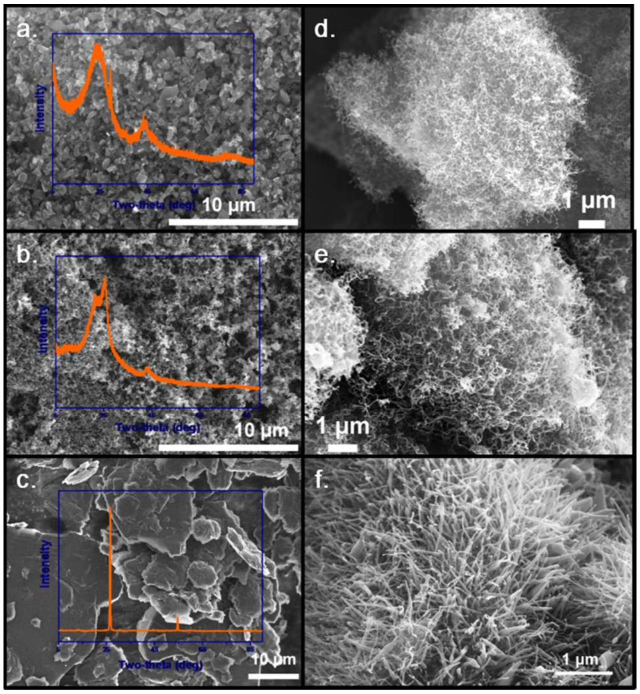

Figure 2 SEM images of the solid carbon sources and their obtained CNTs: (d), (e), and (f) CNTs produced from (a) amorphous carbon powder, (b) carbon black, (c) artificial graphite powder, respectively. The inserted curves are their XRD patterns.

The morphologies of solid carbon precursors and their correspondingly obtained CNT products were measured by SEM, and the images were given in Figure 2. The inserted curves are XRD patterns of three carbon sources. After the water-assisted annealing of carbon/NiO-MgO precursors, CNTs were achieved from various solid carbon sources with different morphologies and crystallinities, indicating the universality of our method. Furthermore, the structures of CNTs can be simply modulated by changing the solid state carbon precursors. In the XRD patterns of the carbon precursors, the broad and dispersive diffraction peaks of both amorphous carbon powder and carbon black demonstrate their low crystalline properties, while the sharp and intensive diffraction peak indicates the high crystallinity of artificial graphite. From the SEM images and the HRTEM images given in Figure 3 e and f, CNTs produced from low crystal carbon precursors of amorphous carbon powder and carbon black exhibit a highly curved morphology and herring-bone type structure, whereas the CNTs from high crystal artificial graphite perform much straight morphology and cylinder type structure. To investigate the detailed growth procedure and structures of the obtained CNTs, we took the CNTs prepared from amorphous carbon powder and artificial graphite as examples and the HRTEM images were provided in Figure 3.

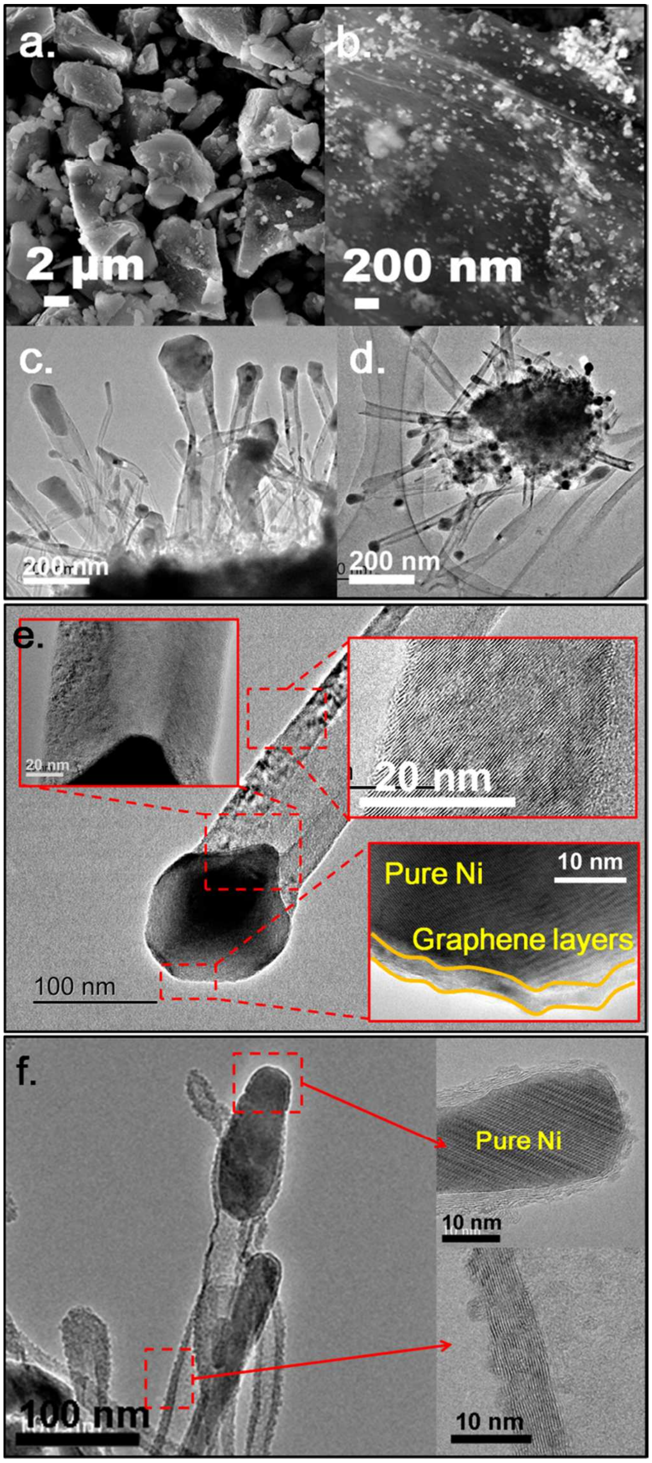

Figure 3 (a) SEM image of the as-prepared catalyst; (b) growth without water vapor using artificial graphite as the precursor; CNTs grown from (c) (e) amorphous carbon powder, and (d) (f) artificial graphite, respectively.

Figure 3a gives the SEM image of the as-prepared NiO-MgO catalyst particle. Without introduction of water vapor, though the Ni nanoparticles can be reduced by artificial graphite (Figure 3b), the growth of CNTs is barely seen in the product. However, the growth of CNTs is clearly observed from both amorphous carbon (Figure 3c) and artificial graphite (Figure 3d) with the introduction of small amount of water vapor into the tubular furnace. The catalyst nanoparticles are located on the tips of the CNTs, demonstrating that their growth follows the typical tip growth mode[19]. In the growth procedure, pure Ni nanoparticles are considered as the active component of the catalyst because they can be clearly identified on the tip of CNTs from the high resolution images given in Figure 3 e and f. What's more, the CNTs prepared from amorphous carbon powder show a herring-bone structure (Figure 3e), which their walls are built up by stacking of small graphene flakes. But the CNTs obtained from high crystalline artificial graphite perform a several layer cylinder-like structure (Figure 3f) which can be seen as the coiling of graphene ribbons. In another words, the morphology and structure of the CNTs can be modulated by simply changing the solid state carbon precursors.

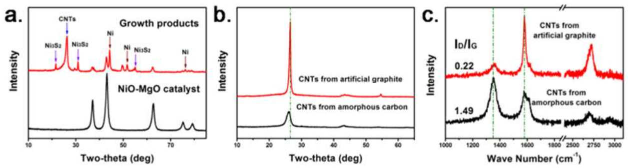

Figure 4 XRD pattern of (a) NiO-MgO catalyst and the growth product, (b) the obtained CNTs from amorphous carbon powder and artificial graphite, (c) Raman spectra of the CNTs from amorphous carbon powder and artificial graphite.

To further understand the growth procedure and the structural properties of the obtained CNTs, XRD and Raman analysis were carried out and the patterns are shown in Figure 4. The as-prepared catalyst exhibits the crystal characteristic of NiO/MgO substitutional solid solution, while pure Ni peaks are clearly seen in the grown products (Figure 4 a). From the mentioned above, the growth process is deduced as that at the beginning, the catalyst particles of NiO-MgO substitutional solid solution were immersed by solid carbon sources. With the rising of treated temperature, Ni was reduced and subsequently active Ni nanoparticles were dissolved out from the NiO-MgO substrate. Due to high reactivity of the acidified carbon sources and strong catalytic activity of the newly formed Ni nanoparticles, active carbon atoms from the solid state carbon covers were gradually absorbed into the Ni nanoparticles, diffused to the opposite side and precipitated out to form CNTs. Therefore, tip growth of CNTs is achieved along with the consumption of the solid phase carbon resources according to this absorption-diffusion-precipitation process[8, 19].

Furthermore, a sharp and intensive peak is seen at 26.5° in the XRD pattern of the CNTs prepared from artificial graphite powder, while a relative broad and weak peak is located at 26° in that of the CNTs obtained from amorphous carbon powder (Figure 4 b), indicating much more ordered stacking of graphene sheets of the cylinder structure than that of the herring-bone one. Raman spectroscopy is a powerful tool to investigate the defect structure of carbon materials. The band located at ca. 1350 cm^{-1} is the D-band which stands for the defects such as vacancy, dislocation, crystal boundary, or edge structure[20-24]. The band located at ca. 1580 cm^{-1} (G-band) stands for the crystal structure from graphitized domains[21, 22, 24]. The 2D-band located at 2700 cm^{-1} indicates the interlayer interaction of the carbon materials[22-

[24]. And the ratio of I_D to I_G given in Figure 4 c indicates the CNTs from amorphous carbon powder exhibit much more defective than that from artificial graphite[21]. Due to the cylinder-like structure with high crystal sidewalls, Raman spectrum of the CNTs from artificial graphite shows very sharp G-band and 2D-band while a weak D-band. However, the CNTs from amorphous carbon powder perform a herring-bone structure which their sidewall is constructed by the stacking of small graphene flakes. Under this circumstance, abundant edge sites are exposed with numerous stacking faults between the small building blocks, resulting in the strong D-band and weak and dispersive G-band and 2D-band in the Raman curves[21-24].

The formation of cylinder-like or herring-bone structure may be due to the crystallinity of the solid carbon precursors. The growth of CNTs follows the adsorption-diffusion-precipitation mechanism, and it is general that the solid carbon performs more reactivity with more disordered structure. During the growth, carbon atoms from amorphous carbon powder are easier to diffuse into the catalyst nanoparticles. The Rapid carbon supersaturation in the catalyst leads to the fast precipitation of carbon atoms on the opposite site. The herringbone type CNTs are thus fabricated with the formation of small graphene flakes. The artificial graphite shows relative low chemical reactivity. The slow diffusion rate of carbon atoms from artificial graphite towards catalyst nanoparticles allow more ordered arrangement of the carbon atoms in the precipitation process, leading to the formation of high crystal cylinder CNTs.

It should be noticed that from the SEM images (Figure 2), the whole catalyst particles were encapsulated by the as-prepared CNT clusters while barely other forms of carbon were detected in these nanotube forests. This phenomenon was further proven by the HRTEM image that only the tip grown CNTs were found on the surface of Ni-MgO particles, thus the solid carbon sources were deduced to mostly transform to CNTs. We reported previously that solid state carbon sources can be transformed into carbon nanofibers at the high temperature of 1500 ˚C without water vapor[10]. Briefly, Fe@C eutectic spheres were initially formed by the reaction between highly oxidized carbon sources and the catalyst of iron nanoparticles in solid phase. After the subsequent diffusion and precipitation of the carbon component throughout the molten metal, carbon nanofibers were fabricated along with the formation of micrometer carbon shells on the surface of the metal spheres. However, there are several differences compared with that of the water-assisted approach: (1) under the relative low temperature of 850 ˚C, both of the catalyst particles and carbon sources remained their solid states, thus the molten micrometer spheres cannot be received; (2) barely carbon shells or other carbon forms but only the CNTs were observed in the product of water-assisted approach. In another words, efficient utilization of low value added carbon sources is achieved in our method to prepare CNTs in solid state.

To achieve the continuous growth of CNTs so as to efficiently utilize of the carbon sources, the catalytic activity of Ni nanoparticles and the reactivity of the solid carbons must be ensured during the fabrication procedure. According to the previous reports, inactivation of the catalyst nanoparticles caused by deposition of amorphous carbon or Ostwald ripening is the dominating problem for its large scale preparation[15-18]. Though masses works have been taken and effective ways such as oxygen-assisted[25], CO_2-assisted[26], and plasma-assisted[27] methods were proposed to overcome this problem, the water-assisted method which was firstly put forward by Iijima et. al.[12] was regarded as the most simple and efficient routes to enhance the activity and catalytic lifetime of the catalysts because trace amount of water vapor can etch the amorphous carbons as well as inhibit the Ostwald ripening of the catalyst nanoparticles[15-18]. Very recently, water-assisted CVD method was also carried out for the preparation of half meter long carbon nanotubes[13, 14]. Here in our works, the Ni nanoparticles maintained their activity till the solid carbon sources were fully transformed to CNTs, thus the tube length is determined by the surrounding solid carbons of the catalyst nanoparticle. Furthermore, even on the tip of the Ni nanoparticle, the deposited carbon displayed highly crystal graphene-like structure as well, barely amorphous carbon was observed in the HRTEM images. As a result, water vapor is deduced to play an important role in keeping the catalytic activity of the Ni nanoparticles, which is much similar in that of CVD method. Besides, water vapor can enhance the reactivity of solid carbons at high temperature by activation[28, 29]. As a consequence, trace amount of water can promote the efficient growth of CNTs by the synergistic effect of (1) elongation the life span of the catalyst and (2) activation the solid carbon sources.

4. Conclusion:

A universal and effective water-assisted approach was developed for the fabrication of CNTs using solid state carbon as the precursors and NiO-MgO as the catalyst. Based on this method, cylinder-like and herringbone-like CNTs are fabricated from artificial graphite and amorphous carbon powder, respectively. Water vapor is considered to play an important role in the growth process. At a relative low temperature of 850 ˚C, trace amount of water could promote the growth of CNTs by maintaining the activity of catalyst and enhancing the reactivity of the solid carbons.

Acknowledgments

This work was supported by the National Natural Science Foundation of China (51202009 and 51272019).

Notes and references

[1] Authors contributed equally to this work.

1 M. F. De Volder, S. H. Tawfick, R. H. Baughman and A. J. Hart, *Science*, 2013, **339**, 535.
2 C. Liu and H.-M. Cheng, *Materials Today*, 2013, **16**, 19.
3 R. H. Baughman, A. A. Zakhidov and W. A. de Heer, *Science*, 2002, **297**, 787.
4 H. Qian, E. S. Greenhalgh, M. S. Shaffer and A. Bismarck, *J. Mater. Chem.*, 2010, **20**, 4751.
5 D. Eder, *Chem. Rev.*, 2010, **110**, 1348.
6 S. Iijima, *Nature*, 1991, **354**, 56.
7 J. Prasek, J. Drbohlavova, J. Chomoucka, J. Hubalek, O. Jasek, V. Adam and R. Kizek, *J. Mater. Chem.*, 2011, **21**, 15872.
8 J. P. Tessonnier and D. S. Su, *ChemSusChem*, 2011, **4**, 824.
9 C. H. See and A. T. Harris, *Ind. Eng. Chem. Res.*, 2007, **46**, 997.
10 Y. Shen, L. Yan, H. Song, J. Yang, G. Yang, X. Chen, J. Zhou, Z. Z. Yu and S. Yang, *Angew. Chem. Int. Ed.*, 2012, **51**, 12202.
11 E. Dervishi, S. Bourdo, J. A. Driver, F. Watanabe, A. R. Biris, A. Ghosh, B. Berry, V. Saini and A. S. Biris, *ACS Nano*, 2011, **6**, 501.

12 K. Hata, D. N. Futaba, K. Mizuno, T. Namai, M. Yumura and S. Iijima, *Science*, 2004, **306**, 1362.
13 R. Zhang, Y. Zhang, Q. Zhang, H. Xie, W. Qian and F. Wei, *ACS Nano*, 2013, **7**, 6156.
14 R. Zhang, Y. Zhang, Q. Zhang, H. Xie, H. Wang, J. Nie, Q. Wen and F. Wei, *Nat. Commun.*, 2013, **4**, 1727.
15 T. Yamada, A. Maigne, M. Yudasaka, K. Mizuno, D. N. Futaba, M. Yumura, S. Iijima and K. Hata, *Nano Lett.*, 2008, **8**, 4288.
16 P. B. Amama, C. L. Pint, L. McJilton, S. M. Kim, E. A. Stach, P. T. Murray, R. H. Hauge and B. Maruyama, *Nano Lett.*, 2008, **9**, 44.
17 N. Yoshihara, H. Ago and M. Tsuji, *J. Phys. Chem. C*, 2007, **111**, 11577.
18 D. N. Futaba, K. Hata, T. Namai, T. Yamada, K. Mizuno, Y. Hayamizu, M. Yumura and S. Iijima, *J. Phys. Chem. B*, 2006, **110**, 8035.
19 S. Sinnott, R. Andrews, D. Qian, A. Rao, Z. Mao, E. Dickey and F. Derbyshire, *Chem. Phys. Lett.*, 1999, **315**, 25.
20 I. Pócsik, M. Hundhausen, M. Koós, L. Ley, *J. Non-Cryst. Solids.*, 1998, **227-230**, 1083.
21 E. B. Barros, N. S. Demir, A. G. S. Filho, J. M. Filho, A. Jorio, G. Dresselhaus, M. S. Dresselhaus, *Phys. Rev. Lett.*, 2005, **71**, 165422.
22 Y. Wang, D. C. Alsmeyer, R. L. McCreery, *Chem. Mater.*, 1990, **2**, 557.
23 M. S. Dresselhaus, A. Jorio, M. Hofmann, G. Dresselhaus, R. Saito, *Nano. Lett.*, 2010, **10**, 751.
24 Z. Ni, Y. Wang, T. Yu, Z. Shen, *Nano. Res.*, 2008, **1**, 273.
25 C. L. Pint, S. T. Pheasant, A. N. G. Parra-Vasquez, C. Horton, Y. Xu and R. H. Hauge, *J. Phys. Chem. C*, 2009, **113**, 4125.
26 A. G. Nasibulin, D. P. Brown, P. Queipo, D. Gonzalez, H. Jiang and E. I. Kauppinen, *Chem. Phys. Lett.*, 2006, **417**, 179.
27 Z. Ren, Z. Huang, J. Xu, J. Wang, P. Bush, M. Siegal and P. Provencio, *Science*, 1998, **282**, 1105.
28 F. Rodriguez-Reinoso, M. Molina-Sabio and M. Gonzalez, *Carbon*, 1995, **33**, 15.
29 M. Molina-Sabio, M. Gonzalez, F. Rodriguez-Reinoso and A. Sepulveda-Escribano, *Carbon*, 1996, **34**, 505.